



Deformation regime and long-term precursors to eruption at large calderas: Rabaul, Papua New Guinea



Robert M. Robertson, Christopher R.J. Kilburn *

UCL Hazard Centre, Department of Earth Sciences, University College London, Gower Street, London WC1E 6BT, UK

ARTICLE INFO

Article history:

Received 6 July 2015

Received in revised form 26 December 2015

Accepted 4 January 2016

Available online xxxx

Editor: T.A. Mather

Keywords:

large caldera

Rabaul

eruption precursors

eruption forecasts

volcano-tectonic seismicity

ground deformation

ABSTRACT

Eruptions at large calderas are normally preceded by variable rates of unrest that continue for decades or more. A classic example is the 1994 eruption of Rabaul caldera, in Papua New Guinea, which began after 23 years of surface uplift and volcano-tectonic (VT) seismicity at rates that changed unevenly with time by an order of magnitude. Although the VT event rate and uplift rate peaked in 1983–1985, eruptions only began a decade later and followed just 27 hours of anomalous changes in precursory signal. Here we argue that the entire 23 years of unrest belongs to a single sequence of damage accumulation in the crust and that, in 1991–1992, the crust's response to applied stress changed from quasi-elastic (elastic deformation with minor fault movement) to inelastic (deformation predominantly by fault movement alone). The change in behaviour yields limiting trends in the variation of VT event rate with deformation and can be quantified with a mean-field model for an elastic crust that contains a dispersed population of small faults. The results show that identifying the deformation regime for elastic-brittle crust provides new criteria for using precursory time series to evaluate the potential for eruption. They suggest that, in the quasi-elastic regime, short-term increases in rates of deformation and VT events are unreliable indicators of an imminent eruption, but that, in the inelastic regime, the precursory rates may follow hyperbolic increases with time and offer the promise of developing forecasts of eruption as much as months beforehand.

© 2016 Elsevier B.V. All rights reserved.

1. Introduction

Large calderas, with surface areas of 100 km² or more, are among the most populated active volcanoes on Earth. At least 138 have records of historical unrest (Newhall and Dzurisin, 1988) and examples that have provoked recent emergencies include Rabaul in Papua New Guinea (McKee et al., 1984; Nairn et al., 1995), Campi Flegrei in Italy (Barberi et al., 1984), Long Valley in the USA (Hill et al., 2002), and Santorini in Greece (Parks et al., 2012). During such emergencies, elevated unrest continues for ~0.1–1 years and is characterised by caldera-wide uplift and volcano-tectonic (VT) events within the caldera to depths of kilometres. Most episodes do not culminate in eruption and their activity has been attributed to a combination of the intrusion of magma at depths of about 5 km or less and increased rates of fluid circulation in near-surface hydrothermal systems (McKee et al., 1984; Battaglia and Vasco, 2006; Geyer and Gottsmann, 2010; Woo and Kilburn, 2010; Bodnar et al., 2007; Parks et al., 2012; Acocella et al., 2015).

* Corresponding author.

E-mail address: c.kilburn@ucl.ac.uk (C.R.J. Kilburn).

Even though short-term emergencies tend to be evaluated independently as regards the probability of eruption (McKee et al., 1984; Hill, 2006), it has long been recognised that they may belong to longer-term unrest that will trigger an eruption only when a cumulative threshold has been exceeded (Newhall and Dzurisin, 1988; De Natale et al., 2006; Hill, 2006; Acocella et al., 2015). However, the connection between long-term unrest and eruption potential has been described only qualitatively. Using data from Rabaul caldera, we argue (1) that VT and deformation precursors at large calderas may belong to a unified sequence that can be quantified over decadal timescales, and (2) that conditions for eruption are determined by the transition from a quasi-elastic to inelastic response of the crust to applied stress. The results confirm that, on their own, short-term changes in rates of unrest are unreliable guides to the potential for eruption. They also identify new practical procedures for evaluating a caldera's approach to eruption.

2. Long-term unrest at Rabaul caldera

Among large calderas, Rabaul has a unique modern record of precursory unrest that lasted for more than two decades, between 1971 and 1994, and included a non-eruptive emergency during 1983–1985 before eruptions began on 19 September 1994.

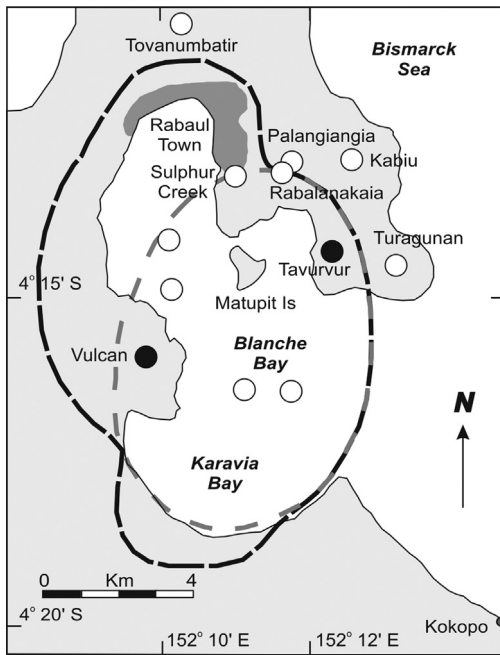


Fig. 1. Map of Rabaul caldera, showing the outlines of the Blanche Bay complex of nested calderas (large black dashes) and of the most recent collapse in 1400 BP (small, grey dashes). The 1971–1994 unrest ended with simultaneous eruptions from Tavorvur and Vulcan (black circles) and provoked evacuation of Rabaul Town. Previous eruptions (white circles) have occurred within and outside the Blanche Bay complex. (Modified from Johnson et al., 2010.)

The caldera lies on the northeastern coast of New Britain Island in Papua New Guinea (Fig. 1). At least five episodes of collapse have occurred since the Late Pleistocene across an area about 14 by 9 km across, most of which is now submerged beneath Blanche Bay and opens eastward into the Bismarck Sea (Nairn et al., 1995). The most recent caldera collapse occurred 1400 years ago (Nairn et al., 1995). It formed an elliptical structure, about 10

by 6.5 km across and aligned approximately North–South, since when andesitic-dacitic eruptions have occurred around its margin at Tavorvur, Vulcan, Rabalanakaia and Sulphur Creek (Fig. 1; Nairn et al., 1995; Wood et al., 1995; Johnson et al., 2010). The historical record dates back to the 18th Century and consists of at least six events, in 1767, 1791, 1850, 1878, 1937–43 and 1994–Present (McKee et al., 1985; Blong and McKee, 1995; Johnson et al., 2010). During the last three eruptions, activity started almost simultaneously at Vulcan and Tavorvur, on opposite sides of the caldera (Fig. 1), with the later stages becoming restricted to Tavorvur (Blong and McKee, 1995).

Unrest before the 1994 eruptions was recognised in late 1971 after 54 years of quiescence (McKee et al., 1984; Mori et al., 1989). Six months after two tectonic earthquakes of local magnitude (M_L) 8.0 had occurred in the Solomon Sea (Everingham, 1975), volcano-tectonic (VT) earthquakes began to be detected at mean rates greater than the previously typical values of 50–100 events per month (McKee et al., 1985). They were located at depths of about 4 km or less and associated with normal and subsidiary reverse fault displacements (Mori and McKee, 1987; Mori et al., 1989; Nairn et al., 1995; Jones and Stewart, 1997; Johnson et al., 2010). Their epicentres were concentrated within the topographic expression of the 1400 BP caldera (Fig. 2), indicating a narrower zone of ring faults at shallow depth (Mori et al., 1989). Approaching 2×10^5 VT events were recorded throughout unrest (Fig. 3). Most had local magnitudes between about 0.5 and 2.0, although their relative frequency could not be determined reliably for the full 23 years of unrest (Mori et al., 1989; Johnson et al., 2010). Among the $\sim 10^4$ VT events recorded during the 1983–85 volcano-seismic crisis, the maximum local magnitude was 5.1 and fewer than one percent had local magnitudes greater than 3.0 (Mori et al., 1989). For unspecified completeness magnitudes, estimates of the seismic b -value during the crisis lie between 0.8 and 1.1 (Mori et al., 1989) and so, assuming a value of 1, fewer than 10% are expected to have had local magnitudes greater than 2.0.

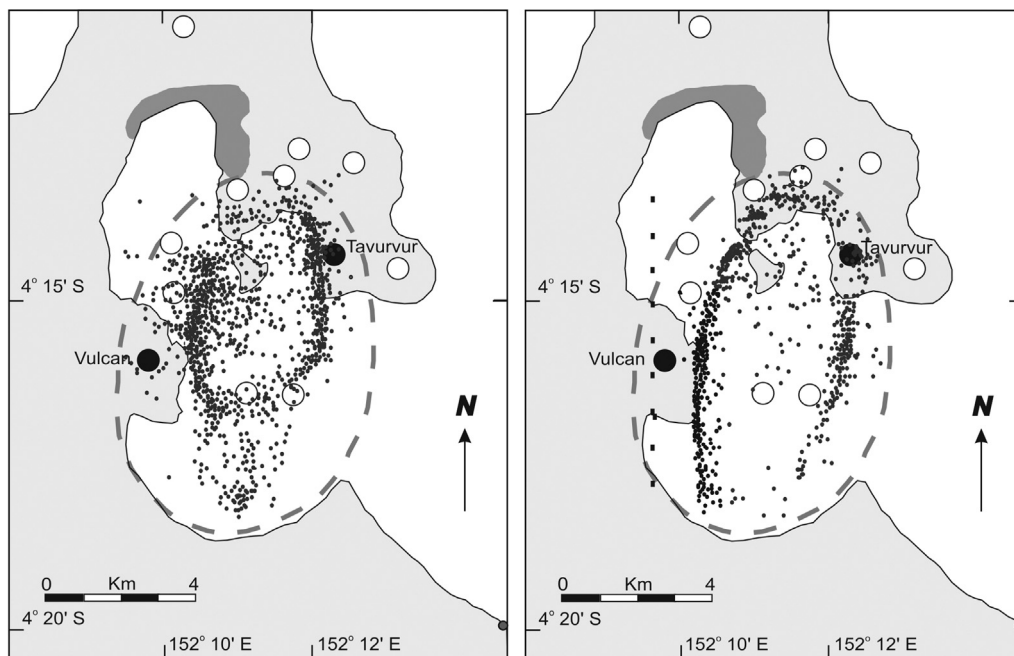


Fig. 2. The distribution of local seismicity recorded during 1971–1992. The VT events occurred at depths of less than 4 km and their epicentres (black dots) appear to mark an inner zone of faults associated with the 1400 BP caldera (grey dashes). Compared with events at depths of 2 km or less (left), the distribution becomes extended towards the south among events deeper than 2 km (right). Tavorvur and Vulcan (black circles) lie outside the outer margin of the more shallow VT events. See Fig. 1 for names of additional locations. (Modified from Jones and Stewart, 1997 and Saunders, 2001.)

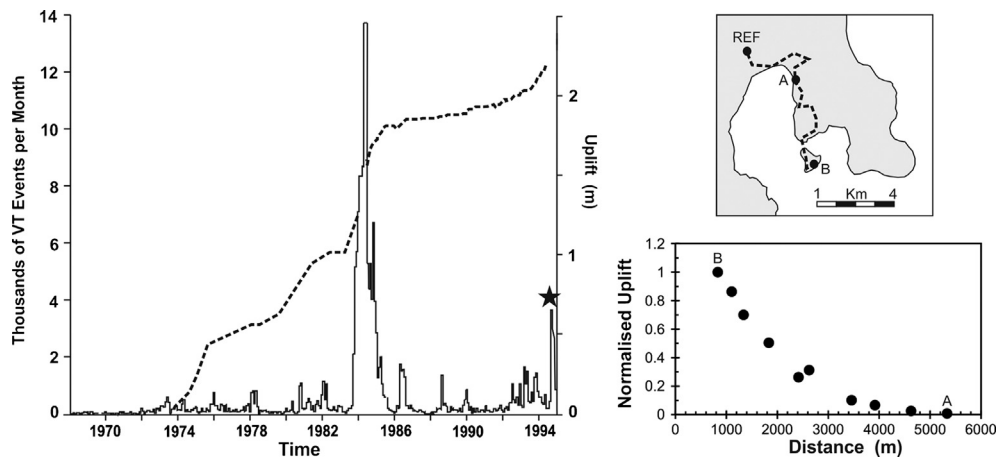


Fig. 3. During the 1971–1994 unrest, the monthly VT event rate (columns) and uplift at Matupit Island (line) both varied irregularly with time (left). The 1983–1985 seismo-volcanic crisis was characterised by increases in rate by at least one order of magnitude, but decayed without an eruption. The eruptions in 1994 (star) were not preceded by anomalous behaviour until 27 hours beforehand and the onset of a seismic swarm that raised the monthly number of VT events to about 3700 and caused uplift near Vulcan and Tauruvur by several metres (not shown). The amount of long-term uplift decayed along the measuring line northward from Matupit Island (top right). REF shows the reference base station and A and B the end stations used to illustrate the pattern of uplift during 1971–1984 (bottom right). The uplift has been normalised against the uplift recorded at Station B on Matupit Island. (Modified from (left) Johnson et al., 2010, (top right) Saunders, 2001 and (bottom right) McKee et al., 1984; note that the times in the original Fig. 46 of Johnson et al., 2010 should be moved earlier by six months.)

Between 1971 and 1994, the VT event rate recorded by the same seismic network (Itikarai, I., pers. comm.) showed mean values of 100–200 per month, rising and falling over intervals of years around peak values from about 600 per month in 1973 to almost 2000 per month in 1993 (Fig. 3; McKee et al., 1985; Itikarai, 2006; Johnson et al., 2010). This trend was interrupted between September 1983 and July 1985 by a surge in monthly numbers that peaked at almost 14,000 (Fig. 3).

From 1973, the changes in VT event rate were accompanied by uplift along a deformation route that ran northwards from Matupit Island (Fig. 3; McKee et al., 1984; Saunders, 2001). The uplift decreased with distance from a maximum value measured on the south coast of the island. Although uplift was recorded over about 6 km, some 80% occurred within 2.5 km of the location of peak movement and is consistent with deformation over a pressure source at a depth of about 2 km (McKee et al., 1984). At Matupit Island itself, the peak rate of uplift varied from about 0.02 to 0.4 m per year, with the largest rates occurring during the early stages of unrest and the 1983–85 peak in VT event rate (Fig. 3; McKee et al., 1984; Blong and McKee, 1995; Saunders, 2001; Johnson et al., 2010).

3. Precursors to eruption

The VT and deformation trends show three remarkable features (Fig. 3). First, their annual rates with time varied by at least one order of magnitude. Second, although both precursors showed high rates during the 1983–85 crisis, their mean rates did not vary in direct proportion for most of the unrest (Fig. 3). Third, although some 40% of the total uplift and number of VT events occurred during 1983–85, this crisis did not culminate in volcanic activity; in contrast, the eventual eruption on 19 September 1994 began without significant changes in the rate of either precursor until 27 hours beforehand, when rates of seismicity increased to peak values of about two felt events per minute and the ground was uplifted by several metres at least near Vulcan and, also, Matupit Island, 2.5 km west of Tauruvur (Global Volcanism Program, 1994a, 1994b; Blong and McKee, 1995); explosive activity finally commenced at 06.05 (local time) at Vulcan and 07.17 at Tauruvur (Global Volcanism Program, 1994a). The first feature shows that unrest at Rabaul occurred under varying rates of deformation and fault movement; the second shows that deformation and VT pre-

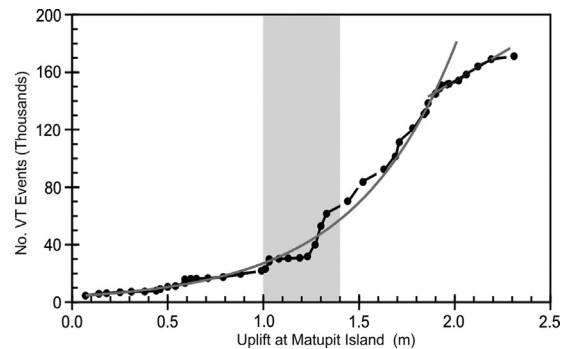


Fig. 4. The variation of VT event number (ΣN) against uplift (h) at Matupit Island shows a change from an exponential to linear trend at an uplift of about 1.9 m. The best-fit relations (for h in m) are $\Sigma N = 4120 \exp(h/0.53)$ and $\Sigma N = 2.79 \times 10^4 + (6.23 \times 10^4)h$, with corresponding r^2 regression coefficients of 0.98 and 0.99. The change in trends are consistent with an evolution from the quasi-elastic to inelastic regimes of deformation (Fig. 5). The shaded area shows conditions during the 1983–1985 seismo-volcanic crisis (Fig. 3).

cursors do not necessarily show the same types of variation with time; and the third shows that, on their own, accelerations in precursor signals with time may not be sufficient for assessing the potential for eruption.

Even when deformation and VT seismicity show contrasting behaviour with time, they are expected to show preferred variations against each other, because both are responses of the crust to changes in applied stress (Kilburn, 2012). In the case of Rabaul, Fig. 4 shows the variation of VT events with uplift for the entire period of unrest before the 1994 eruption. Following previous studies, uplift is represented by measurements from Matupit Island, where the maximum amount of movement was recorded (McKee et al., 1984, 1989; Blong and McKee, 1995; Johnson et al., 2010), although geodetic models suggest that the measured value may have been about 85% of the potential absolute maximum towards the centre of the caldera offshore (McKee et al., 1984).

The data show coherent trends between VT event number and uplift (Fig. 4). Qualitatively, the number of VT events tends to accelerate with deformation for uplifts less than c. 1.9 m (from 1973 to the end of 1988), followed by a transition to a linear trend for uplifts larger than 2 m (from at least December 1991 to September 1994). The accelerating phase may belong to a single trend or be

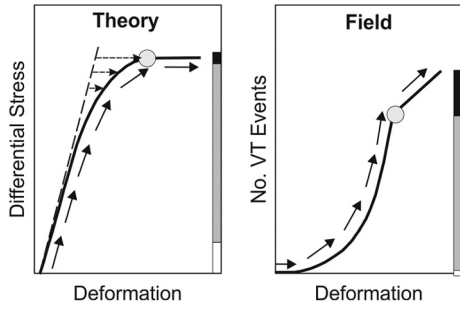


Fig. 5. As the applied differential stress increases (left), the deformation of an elastic–brittle material (black curve) deviates by an increasing amount (horizontal dashed arrows) from ideal elastic behaviour (dashed line). The deviation is caused by fracturing and slip along discontinuities. The rate of stress increase is eventually balanced by the rate of stress loss by slip (circle), after which deformation continues only by slip and the mean stress remains constant at its failure value S_F . The change in regime is recorded in the field (right) by a change from an accelerating to a constant rate of change in VT event number with total deformation. The vertical bars illustrate conditions for elastic (white), quasi-elastic (grey) and inelastic (black) behaviour. The continuous arrows show the direction of evolution with time under an increasing stress. The expected field trends are observed during the 1971–1994 unrest at Rabaul (Fig. 4).

composed of a non-linear increase for uplifts less than c. 1.2 m and a quasi-linear increase for uplifts between 1.2 and 1.9 m, at a mean rate faster than that for the uplift beyond 1.9 m. On its own, therefore, simple curve fitting cannot provide a unique interpretation of the VT-deformation trends. However, as described in the next section, a preferred interpretation does naturally emerge when additional constraints from elastic–brittle deformation are taken into account.

4. Regimes of deformation

4.1. Limiting regimes of deformation

The emergence of different trends in Fig. 4 suggests an evolution in conditions controlling Rabaul's deformation. The number of VT events and uplift are proxies, respectively, for inelastic and total deformation of the crust. The field trend can thus be interpreted in terms of the variation with deformation in the contribution from inelastic behaviour and this, in turn, can be represented on a conventional stress–strain diagram for an elastic–brittle crust (Fig. 5). When a differential stress is applied (e.g., from overpressure in a magma body), the crust ideally first responds elastically, so that the stress is supported by straining unbroken rock. Above a critical differential stress, a proportion of the stress is lost inelastically by the onset of fault slip (Fig. 5). The inelastic proportion increases with stress at an accelerating rate until it becomes the sole mode of response (Fig. 5). The rates of stress increase and loss eventually balance each other, so that the mean differential stress remains unchanged (Fig. 5). At this stage, the total rate of deformation is determined by the rate of faulting, favouring a linear increase between measures of deformation and seismicity. The field trends at Rabaul (Fig. 4) are qualitatively similar to the evolution in deformation regime; the conditions for elastic–brittle behaviour may therefore yield also a quantitative description of the caldera's unrest.

Rabaul's VT events have typical magnitudes of less than 2 and record the movements of faults ~ 0.01 – 0.1 km across, much smaller than the dimensions of \sim km of the deforming crust. The crust's bulk behaviour can thus be approximated to that of an elastic medium containing a dispersed population of relatively small faults. The rate of faulting is governed by slow crack growth around fault tips. Until a critical rate is achieved, continued cracking requires an increase in applied stress, as observed for quasi-elastic deformation (Kilburn, 2012); at faster rates, crack growth becomes

a self-accelerating process even when the applied stress remains constant, as expected in the inelastic regime (Kilburn, 2003). Bulk deformation can therefore be described by a mean-field model for a crust with a population of small faults that slip at rates determined by slow crack growth (Kilburn, 2003, 2012).

4.2. Quasi-elastic deformation

For the quasi-elastic regime, the mean-field, slow-crack model yields an exponential increase in the mean inelastic deformation, ε_{in} , with total mean deformation, ε_t (Kilburn, 2012):

$$\frac{d\varepsilon_{in}}{d\varepsilon_t} = \left(\frac{d\varepsilon_{in}}{d\varepsilon_t} \right)_{st} \exp\left(\frac{\varepsilon_t - \varepsilon_{QE,m}}{\varepsilon_{ch}} \right) \quad (1)$$

where $\varepsilon_{QE,m}$ is the total mean deformation at the end of quasi-elastic behaviour, when $d\varepsilon_{in}/d\varepsilon_t = (d\varepsilon_{in}/d\varepsilon_t)_{st}$, and ε_{ch} is a characteristic deformation. Setting the total number of VT events $\Sigma N \propto \varepsilon_{in}$ and uplift $h \propto \varepsilon_t$, Eq. (1) becomes:

$$\frac{dN}{dh} = \left(\frac{dN}{dh} \right)_0 \exp\left(\frac{h}{h_{ch}} \right) \quad (2)$$

where $(dN/dh)_0 = (dN/dh)_{st} \exp(-h/h_{ch})$ is the value of dN/dh at the onset of significant quasi-elastic behaviour, for which h is set at 0. (Note that some uplift is expected to have occurred before the onset of the exponential trend, so that $h = 0$ in Eq. (2) corresponds to finite initial uplift in the field.) Integrating Eq. (2) with uplift then leads to

$$\Sigma N = (\Sigma N)_0 \exp\left(\frac{h}{h_{ch}} \right) \quad (3)$$

where $(\Sigma N)_0$ denotes the number of VT events detected at $h = 0$. Eq. (3) is consistent with observations at Rabaul for uplifts less than 1.9 m, yielding best-fit values of $(\Sigma N)_0$ and h_{ch} of 4120 events and 0.53 m (Fig. 4). The agreement supports the interpretation that a single VT-deformation trend characterised this phase and reflects early deformation of the caldera's crust in the quasi-elastic regime.

The model further provides an upper limit on the quasi-elastic value for h/h_{ch} . The total quasi-elastic strain increases approximately in proportion with stress. The assumption that $h \propto \varepsilon_t$, therefore leads to $h/h_{ch} \approx S_d/S_{ch}$, the ratio of applied differential stress to a characteristic stress, defined below. The maximum quasi-elastic value for h/h_{ch} then represents S_F/S_{ch} , where S_F is the differential failure stress of the crust appropriate to the particular conditions of loading (e.g., in compression or extension). S_{ch} is the stress potentially available to deform bonds as a result of fluctuations in atomic configuration (Kilburn, 2012). Its value depends on the mode of deformation. For shear failure in compression, it is equivalent to the maximum value $S^* = (3kT\phi + P_c - P_p)/3$, where T is absolute temperature (K), P_c and P_p are the confining and pore-fluid pressures, k is the Boltzmann constant (1.381×10^{-23} J molecule $^{-1}$ K $^{-1}$) and ϕ is the number of molecules per unit volume, which in turn depends on rock chemistry and density (Kilburn, 2012). Failure in tension, however, is limited only by the smaller stress necessary to pull bonds apart, equivalent to the tensile strength σ_T . For extension, therefore, $S_{ch} = \sigma_T < S^*$ and is the preferred characteristic stress for a crust stretching during uplift.

Different modes of failure are associated with specific ranges for the ratio S_F/σ_T (Shaw, 1980). In an extending crust, $S_F/\sigma_T \leq 4$ for failure in tension, but lies between 4 and 5.5 for failure in combined tension and shear; in comparison, $S_F/\sigma_T > 5.5$ for failure in compression (Shaw, 1980). At Rabaul, a maximum quasi-elastic uplift of 1.9 m was recorded at Matupit Island (Fig. 4), with a potential maximum of 2.2 m near the presumed centre of uplift offshore. Given $h_{ch} = 0.53$ m, therefore, the maximum value for

h/h_{ch} yields the range 3.6–4.1 for S_F/σ_T , further supporting the interpretation of quasi-elastic crustal extension for the exponential VT-uplift trend.

4.3. Inelastic deformation

In the inelastic regime, changes in total deformation are determined only by fault movement, so that measures of total and inelastic deformation increase in proportion to each other. The substitute parameters uplift and VT event number also increase together to yield a linear trend:

$$\Sigma N - (\Sigma N)_{i,0} = (dN/dh)_i (h - h_{i,0}) \quad (4)$$

where the gradient $(dN/dh)_i$ is the change in VT event number per unit uplift and the subscript “ $i, 0$ ” denotes values at the start of the inelastic regime. Such a trend well describes the VT-deformation behaviour at Rabaul for uplifts greater than 2 m and yields a best-fit gradient of 6.23×10^4 events per metre (Fig. 4). The change from an exponential to a linear trend is thus consistent with the transition from quasi-elastic to inelastic deformation of Rabaul’s crust.

Under the constant applied stress of the inelastic regime, the mean field model shows that the approach to bulk failure is characterised by mean rates of inelastic and total deformation that accelerate hyperbolically with time (Kilburn, 2003), equivalent to a linear decrease in the inverse event rate:

$$\left(\frac{d\varepsilon_{in}}{dt}\right)^{-1} = \left(\frac{d\varepsilon_t}{dt}\right)^{-1} = \left(\frac{d\varepsilon_t}{dt}\right)_1^{-1} \left[1 - \left(\frac{t-t_1}{\tau}\right)\right] \quad (5)$$

where $(d\varepsilon_t/dt)_1 = (d\varepsilon_{in}/dt)_1$ denotes the mean deformation rate at the start of the hyperbolic trend, when time $t = t_1$. The timescale τ defines the duration of the trend, which depends on the failure strength of the crust and the rate of stress concentration around fault tips (Kilburn, 2003).

The corresponding trends for changes in the mean rates of deformation and VT number will show the same form as Eq. (5). For example, the inverse deformation rate is given by:

$$\left(\frac{dh}{dt}\right)^{-1} = \left(\frac{dh}{dt}\right)_1^{-1} \left[1 - \left(\frac{t-t_1}{\tau}\right)\right] \quad (6)$$

which has a linear gradient of $-1/(\tau(dh/dt)_1)$.

The inelastic trend had become established by the beginning of 1992, when uplift at Matupit Island had reached 2 m (Fig. 4). Fig. 6 shows the associated inverse mean rate of uplift, derived from interpolations of the uplift data in Blong and McKee (1995) and Johnson et al. (2010) until the last date of published measurements in March 1994. The mean inverse rates rapidly settle to a trend that for at least 680 days is well-approximated by a linear decrease with time following a best-fit gradient of 14.4 days m^{-1} . The trend thus supports the interpretation that, by the start of 1992, Rabaul’s crust had entered an inelastic regime of deformation controlled by self-accelerating crack growth.

Manipulating Eq. (6), the hyperbolic increase in contemporaneous VT event rate is:

$$\left(\frac{dN}{dt}\right) = \left(\frac{dN}{dh}\right) \left(\frac{dh}{dt}\right) = \left(\frac{dN}{dh}\right) \left(\frac{dh}{dt}\right)_1 \left[1 - \left(\frac{t-t_1}{\tau}\right)\right]^{-1} \quad (7)$$

where the rate of change of VT event number with uplift, dN/dh , is assumed to be constant at 6.23×10^4 events m^{-1} , given by the mean gradient of the inelastic trend line in Fig. 4.

Fig. 6 compares the observed and calculated variations in VT event number with time. The two trends agree well during the start of the inelastic regime, but begin to diverge after about 11 months. At this time, the rate of increase in event rate with time

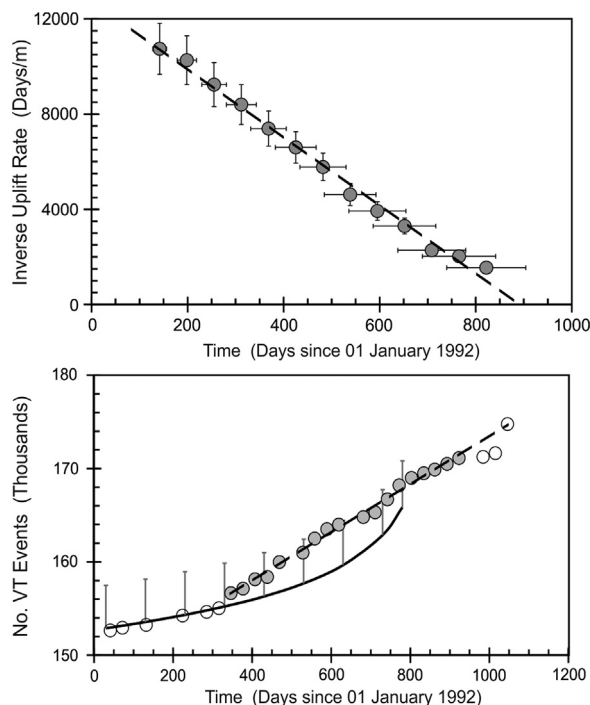


Fig. 6. The inverse mean rate of uplift $\Delta t/\Delta h$ decays linearly with time t (top) during the 1992–1994 inelastic deformation at Rabaul (Fig. 4). The best-fit trend is described by $\Delta t/\Delta h = 12784 - 14.38t$ ($r^2 = 0.99$; h in m and t in days from 01 January 1992); the bars show $\pm 10\%$ limits about the mean value. For ideal inelastic behaviour, the deformation trend yields an acceleration in contemporaneous VT event number with time (bottom, black curve). Observed VT event numbers follow the expected trend until Day 320, after which they instead follow a constant rate of increase (dashed line, fit using only the shaded circles). The deviation may be caused by the progressive opening of ring faults (Fig. 7). The vertical bars illustrate a 3% increase above the VT numbers calculated from the deformation trend.

changes from hyperbolic to approximately constant, yielding values as much as 3% greater than expected from the calculated trend (Fig. 6). Although the difference in values is small enough to give an approximate proportionality between ΣN and h in Fig. 4, the difference suggests a systematic deviation from the expected trend.

Relaxing the assumption that dN/dh is constant, Eq. (7) shows that a linear increase in VT number could be produced if dN/dh decreased with time to counterbalance the acceleration in dh/dt . A decrease in dN/dh is equivalent to an increase in the amount of uplift per fault movement. Two mechanisms favouring such a condition are the coalescence of faults and the opening of discontinuities much larger than the faults triggering VT events. In the first case, the coalescence of faults would yield an increase in the average magnitude of VT events, so reducing the number of events associated with a given amount of uplift (Meredith et al., 1990). In the second case, upward bending of the crust around a magma body (Pollard and Johnson, 1973) would favour the progressive opening of pre-existing, sub-vertical discontinuities in the ring-fault system, as well as an upward migration in the depth at which opening can occur (Fig. 7). Slip in the crust around zones of opening would not necessarily require any coalescence of faults and so not lead to a significant change in the average magnitude of VT events. At the same time, opening of the discontinuities themselves need not generate significant seismicity, because tensile stresses normal to the plane of a discontinuity do not favour slip along its length (Troise et al., 1997).

A decrease in dN/dh would produce total numbers of events smaller than those expected from the calculated trend and, by itself, cannot account for the observed increase above the expected values. Larger numbers of VT events could be obtained by an increase in the total number of faults being activated around the

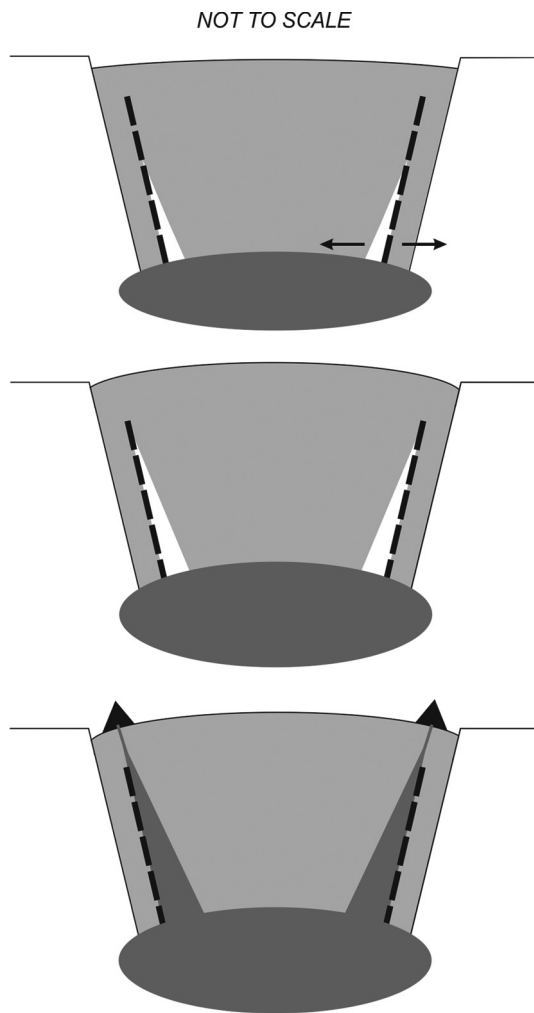


Fig. 7. Bending of crust (light grey) around a pressurising magma body (dark grey) favours the inward opening of weak zones (white) within a caldera's system of ring faults (dashed lines). As bending proceeds (top to bottom), the zone of opening extends towards the surface and, when the walls of the magma body are breached, favours the ascent of magma and its eruption at the surface. The opening migrated slowly upwards during the 1992–1994 interval of inelastic deformation, but was only utilised by ascending magma about 1–2 days before eruption.

caldera rim. Coalescence would favour a decrease in fault number (Smith and Kilburn, 2010), whereas growth of a large discontinuity would favour an increase in the number of smaller faults activated in its vicinity. Qualitatively, therefore, the deviation of VT event numbers from the idealised inelastic trend may reflect the onset of significant stretching and upward opening of the ring-fault system around the rim of the caldera. An opening fault would in addition provide an initial pathway from which magma escaping from the shallow reservoir could force its way to the surface (Fig. 7). Indeed, the propagation of magmatic fractures could account for the increases in local seismicity and uplift observed during the 27 hours before the start of the 1994 eruptions (Global Volcanism Program, 1994b; Blong and McKee, 1995).

Saunders (2001) has also proposed that Rabaul's deformation was controlled by the ascent of magma through caldera ring faults. Magma was considered to have been forcefully injected into faults throughout unrest, generating an overpressure in the resulting dykes that induced lateral compression and associated uplift of the caldera floor. Such a mechanism is distinct from the current interpretation, in which overpressure in a magma reservoir favours surface uplift and inward bending of the crust near the reservoir until the ring faults open sufficiently to favour magma ascent (Fig. 7).

5. Discussion

5.1. The shallow magmatic system at Rabaul caldera

The 1994 eruptions at Rabaul were preceded by a progressive extension of the caldera's crust from at least 1971. During 1991–1992, the style of deformation evolved from quasi-elastic to inelastic, as shown by the following: (1) the VT event number increased at first exponentially and then linearly with uplift (Fig. 4), (2) the transition between trends occurred when the inferred ratio of applied stress to tensile strength was approximately 4, and (3) the final inelastic behaviour was characterised by a linear decrease with time in the inverse mean rate of uplift, equivalent to a hyperbolic increase in the mean rate of deformation (Fig. 6).

The onset of bulk failure is expected to have occurred at or near the margin of a magma body, either through the equivalent of hydraulic failure of the body itself, or by the opening of a major discontinuity at the caldera's boundary. In either case, the recorded VT events reflect slip along small faults in the crust surrounding the magma body or major discontinuity.

In the case of hydraulic failure, the maximum compressive stress (σ_1) at the margin of the magma body is the sum $P_{e,0} + \Delta P_m$ of the effective confining pressure (the confining pressure – pore-fluid pressure) at the start of deformation and the overpressure imposed by the magma body (Gudmundsson, 2011a). Opening of a ring fault may instead occur as the crust of the uplifting caldera is pulled inwards and away from its periphery (Fig. 7), in which case $\sigma_1 \approx P_{e,0}$. For crustal failure in extension, therefore, it is expected that $\sigma_1 \geq P_{e,0}$ which, assuming initially lithostatic conditions, is given by $\rho_{cr}gz$ and $\rho_{cr}(1 - (\rho_f/\rho_{cr}))gz$ for dry and fluid-saturated crust, where ρ_{cr} and ρ_f are the mean density of the crust and pore fluid, g is gravity and z is the depth at which failure begins. The corresponding differential stress, $S_d \approx \sigma_1 + \sigma_T$, which gives $S_d/\sigma_T = (\sigma_1/\sigma_T) + 1$. Since inelastic deformation occurs under the differential stress established at the end of the quasi-elastic regime, the maximum value of S_d/σ_T is 3.6–4.1, so that σ_1 lies between $2.6\sigma_T$ and $3.1\sigma_T$ or, for a notional tensile strength of 10 MPa, in the range 26–31 MPa. For a crust with an assumed mean density of 2200 kg m^{-3} and an aqueous pore-fluid with a density of 1000 kg m^{-3} , pressures of 26–31 MPa correspond to maximum depths of c. 1.2 km and 2.6 km for dry and water-saturated conditions. Given that most of the caldera lies under water (Fig. 1), the preferred solution is for a fluid-saturated crust with a pressure source at depths of less than 2.6 km, consistent with the geodetic modelling of McKee et al. (1984) and Geyer and Gottsmann (2010).

Remarkably, the types of deformation regime are revealed by the numbers of VT events and uplift as simple measures of seismicity and deformation. No filtering has been applied, for example, to select VT events within a prescribed range of completeness magnitudes. Throughout unrest, therefore, the proxy measures appear to have remained in the same relative proportion to the amounts of inelastic and elastic deformation and imply that, at Rabaul: (1) the bulk mechanical behaviour of the crust can be approximated to that of a medium containing a dispersed population of relatively small discontinuities; (2) the magnitude-frequency distribution of VT events remained approximately constant; and (3) the essential geometry of deformation also remained approximately constant.

5.2. Applications to large calderas in general

The evolution from quasi-elastic to inelastic deformation is expected to be common during long-term unrest at large calderas. Conditions for recognising the evolution were particularly favourable at Rabaul because uplift continued throughout unrest to

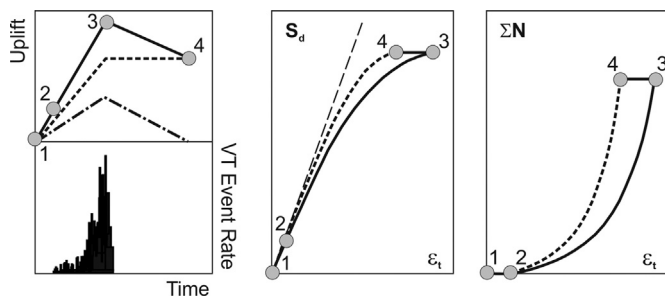


Fig. 8. (Left) Changes in the pore-fluid pressure of hydrothermal systems may produce transient variations in ground movement (dot-dashed line) in addition to the sustained deformation caused by the pressurisation or intrusion of an underlying magma body (dashed line). The transient movements must be removed from the total observed deformation (black line) before the elastic–brittle model can be applied. The example shows uplift accompanied by seismicity, followed by aseismic subsidence as the thermal pulse decays and the pore-fluid pressure in the hydrothermal system decreases to its pre-intrusion level. (Centre and right) The later-stage decrease in pore-fluid pressure is revealed on stress-strain ($S_d - \epsilon_t$) and total seismicity-strain ($\Sigma N - \epsilon_t$) diagrams by a decrease in strain under constant differential stress and without significant seismicity (Positions 3 to 4), here illustrated for deformation in the quasi-elastic regime. Removing the transient movement reveals the elastic–brittle trends associated with changes in differential stress alone (dashed curves from Positions 1 to 2 to 4).

provide a simple measure of increasing deformation. Other large calderas may instead show alternating episodes of uplift and subsidence over years to decades, such as at Campi Flegrei in southern Italy (Piochi et al., 2013) and Yellowstone in Wyoming, U.S.A. (Dzurisin, 2007). Such short-term oscillations must be removed from the total amount of ground movement before the elastic–brittle model can be applied to the sustained, long-term changes in crustal deformation.

Short-term oscillations have been attributed to changes in pore-fluid pressure in shallow hydrothermal systems heated by underlying magma or magmatic gases (Fournier, 1989; Troiano et al., 2011). Changes in pore-fluid pressure alter the isotropic confining pressure on rock (Secor, 1965) and, hence, the total volume of the crust on which a differential stress is being applied. They allow ground movement to occur without altering the magnitude of either the applied differential stress or the difference between total and elastic deformation. Ideally, therefore, increases and decreases in pore-fluid pressure can induce ground uplift and subsidence without changing the applied differential stress or triggering significant additional seismicity (notice that the ideal conditions do not refer to fluids becoming pressurised within existing fractures, which will instead promote fracture growth and attendant seismicity).

Increased pore pressure, however, also reduces the differential stress at which bulk failure occurs (Secor, 1965) and this reduction may trigger additional fracturing. Hence the idealised case of aseismic ground movement following a change in pore pressure implicitly assumes that induced changes in failure stress can be neglected. Such pre-failure behaviour can be recognised on a VT-deformation diagram by abrupt changes in deformation without a change in the total number of VT events (Fig. 8). Once recognised, the movement due to changes in pore-fluid pressure can be removed before applying the elastic–brittle model to the remaining, sustained deformation caused by changes in differential stress (Fig. 8).

Deviations from model conditions will also occur if the crust develops a rheology outside elastic–brittle conditions. For example, Di Luccio et al. (2015) have suggested that long-term exposure to high temperatures may allow the emergence of plastic deformation, which would favour surface movement under a constant differential stress with fewer VT events than expected from the elastic–brittle model. The significance of such processes will vary among calderas and so needs to be evaluated on a case-by-case ba-

sis. By virtue of its simplicity, the elastic–brittle sequence provides a reference model with which to compare observed patterns of unrest and, when significant deviations from the model are observed, to provide a starting point for identifying the physical causes of the deviations.

5.3. Forecasting intra-caldera eruptions after long repose intervals

The elastic–brittle trends show how the regime of crustal deformation evolves during the approach to bulk failure, independent of the time required for stress and strain to be accumulated. Although eruptions after extended repose are normally preceded by bulk failure, this does not mean that all episodes of bulk failure are followed by eruptions (Bell and Kilburn, 2011). Failure may produce a major discontinuity in the crust that does not intersect a magma body; even when magma does enter a new discontinuity, structures in the crust may favour the emplacement of a sill, rather than a dyke (Gudmundsson, 2011b; Woo and Kilburn, 2010), and, in the second case, magmatic pressure gradients may be too small to allow the fracture to reach the surface (Gudmundsson, 2002). Precursory sequences may thus culminate in a seismic swarm or intrusion, instead of an eruption. However, given that an eruption might occur, the analysis of Rabaul’s precursory sequence has identified new procedures for evaluating the possibility of such an outcome.

First, the potential for eruption depends on the proportion of inelastic behaviour during deformation. In addition to monitoring changes in seismic and geodetic precursors with time, therefore, it is important to follow changes in VT event number with a measure of deformation to determine the regime of crustal deformation.

Second, an eruption is most likely to occur after the transition to inelastic behaviour. The transition can be recognised by a change from an exponential to a linear trend in the variation of VT event number with deformation; additional support for a physical change can be obtained from the maximum value of the deformation ratio (in this case h/h_{ch}) at the end of quasi-elastic behaviour, which for deformation in tension is not expected to exceed 4.

Third, when inelastic behaviour has been identified, an accelerating approach to bulk failure can be tested by checking for linear decreases in the inverse mean rates of deformation or VT event number with time, following the classic method of Voight (1988). The preferred time for eruption occurs when the inverse mean event rate becomes zero, because this is equivalent to an approach to infinite rates and is interpreted to mark a catastrophic change in the crust, such as bulk failure. At Rabaul, however, simple extrapolation of the inverse-rate of deformation between January 1992 and March 1994 (Fig. 6) would have indicated a preferred time for eruption at the beginning of June 1994, three months before it actually occurred. Thus, although the linear trend indicates deformation in the inelastic regime, additional analyses may be necessary before it can be utilised to make a specific forecast of an eruption (Bell et al., 2013; Boué et al., 2015). Nevertheless, a sustained linear decrease in the inverse mean rate of deformation may justify a progressive raising of alert levels in the vicinity of a caldera.

Finally, the long-term evolution of the precursory sequence confirms that short-term accelerations in individual precursors are not reliable indicators of an imminent eruption. Instead, they reflect short-duration increases in the rate at which the crust is evolving along the much longer term trend required before an eruption can occur. Thus the 1983–85 crisis at Rabaul represents a two-year acceleration along a trend destined to last for 23 years (Fig. 4). The acceleration is associated with a rapid pressure increase in the magmatic system (McKee et al., 1984), perhaps caused by the injection of magma into a shallow reservoir following a regional earthquake of Magnitude 7.6 in March 1983, 200 km east of the caldera (Accella et al., 2015).

The long precursory sequence contrasts with observations at stratovolcanoes, for which precursory trends tend to evolve over a year or less (Voight, 1988; De La Cruz-Reyna and Reyes-Dávila, 2001; Kilburn, 2003; Bell and Kilburn, 2011). Short-term accelerations of precursory signal with time thus have different implications for eruption potential at stratovolcanoes and at large calderas, so that experience from one cannot be translated to the other without first establishing whether a volcano is deforming in the quasi-elastic or inelastic regime. Time-dependent protocols for emergency responses at large calderas are therefore expected to be significantly different from those at stratovolcanoes.

6. Conclusions

The 1994 eruptions at Rabaul were preceded by a single sequence of unrest that continued for 23 years, during which crustal deformation evolved from the quasi-elastic to inelastic regimes. Upward bending of the crust favoured the opening of ring faults that provided weakened zones for magma to reach the surface. The change in regime was shown by a change from an exponential to a linear increase in the VT event number against uplift, which indirectly measured changes in inelastic against total deformation. Shorter-term accelerations with time in precursory signals provided unreliable indications of the potential for eruption: rapid changes in 1983–85 were not followed by eruption, whereas unremarkable changes in 1994 culminated in simultaneous eruptions at Tavurvur and Vulcan, on different sides of the caldera. Additional measurements that identify the regime of deformation will improve assessments of eruption potential and may reduce the possibilities of false alarms or failed forecasts.

Rabaul's 1971–1994 sequence provided a particularly clear example of the change from quasi-elastic to inelastic behaviour, because unrest was characterised by persistent uplift. At other calderas, uplift may be interrupted by episodes of subsidence, owing to the effects of local processes such as changes in pore-fluid pressures in geothermal systems. In such cases, the effects of local processes must be filtered out before patterns of surface movement and seismicity can be used to identify the regime of deformation.

Acknowledgements

We would like to thank Russell Blong, Doug Finlayson, Ima Itikarai, Wally Johnson, Herman Patia and Steve Saunders for their generous support in providing data and information on unrest at Rabaul. Maurizio Battaglia and an anonymous reviewer helped to improve an earlier version of the text. The research was privately funded.

References

Acocella, V., Di Lorenzo, R., Newhall, C., Scandone, R., 2015. An overview of recent (1988–2014) caldera unrest: knowledge and perspectives. *Rev. Geophys.* 53. <http://dx.doi.org/10.1002/2015RG000492>.

Barberi, F., Corrado, G., Innocenti, F., Luongo, G., 1984. Phlegraean Fields 1982–1984. Brief chronicle of a volcano emergency in a densely populated area. *Bull. Volcanol.* 47, 175–185.

Battaglia, M., Vasco, D., 2006. The search for magma reservoirs in Long Valley Caldera: single versus distributed sources. In: De Natale, et al. (Eds.), *Mechanisms of Activity and Unrest at Large Calderas*. In: *Geol. Soc. (Lond.) Spec. Publ.*, vol. 269, pp. 173–180.

Bell, A.F., Kilburn, C.R.J., 2011. Precursors to dyke fed eruptions at basaltic volcanoes: insights from patterns of volcano-tectonic seismicity at Kilauea Volcano, Hawaii. *Bull. Volcanol.* 74, 325–339.

Bell, A.F., Naylor, M., Main, I.G., 2013. Convergence of the frequency-size distribution of global earthquakes. *Geophys. Res. Lett.* 40. <http://dx.doi.org/10.1002/grl.50416>.

Blong, R., McKee, C.O., 1995. *The Destruction of a Town: The Rabaul Eruption 1994*. Macquarie University NSW, Australia.

Bodnar, R.J., Cannatelli, C., De Vivo, B., Lima, A., Belkin, H.E., Milia, A., 2007. Quantitative model for magma degassing and ground deformation (bradyseism) at Campi Flegrei, Italy: implications for future eruptions. *Geology* 35, 791–794.

Boué, A., Lesage, P., Cortés, G., Valette, B., Reyes-Dávila, G., 2015. Real-time eruption forecasting using the material Failure Forecast Method with a Bayesian approach. *J. Geophys. Res.* 120. <http://dx.doi.org/10.1002/2014JB011637>.

De la Cruz-Reyna, S., Reyes-Dávila, G.A., 2001. A model to describe precursory material-failure phenomena: applications to short-term forecasting at Colima volcano, Mexico. *Bull. Volcanol.* 63, 297–308.

De Natale, G., Troise, C., Pingue, F., Mastrolorenzo, G., Pappalardo, L., Battaglia, M., Boschi, E., 2006. The Campi Flegrei caldera: unrest mechanisms and hazards. In: Troise, C., De Natale, G., Kilburn, C.R.J. (Eds.), *Mechanisms of Activity and Unrest at Large Calderas*. In: *Geol. Soc. (Lond.) Spec. Publ.*, vol. 269, pp. 25–45.

Di Luccio, F., Pino, N.A., Piscini, A., Ventura, G., 2015. Significance of the 1982–2004 Campi Flegrei seismicity: pre-existing structures, hydrothermal processes and hazard assessment. *Geophys. Res. Lett.* 42, 7498–7506. <http://dx.doi.org/10.1002/2015GL064962>.

Dzurisin, D., 2007. *Volcano Deformation*. Springer-Praxis. 441 pp.

Everingham, I.B., 1975. Faulting associated with the Major North Solomon Sea Earthquakes of 14 and 26 July 1971. *J. Geol. Soc. Aust.* 22, 61–70.

Fournier, R.O., 1989. Geochemistry and dynamics of the Yellowstone National Park hydrothermal system. *Annu. Rev. Earth Planet. Sci.* 17, 13–53.

Geyer, A., Gottsmann, J., 2010. The influence of mechanical stiffness on caldera deformation and implications for the 1971–1984 Rabaul uplift (Papua New Guinea). *Tectonophysics* 483, 399–412.

Global Volcanism Program, 1994a. Report on Rabaul (Papua New Guinea). In: Wunderman, R. (Ed.), *Bull. Glob. Volcanism Netw., Smithsonian Institution* 119 (8). <http://dx.doi.org/10.5479/si.GVP.BGVN199408-252140>.

Global Volcanism Program, 1994b. Report on Rabaul (Papua New Guinea). In: Venzke, E. (Ed.), *Bull. Glob. Volcanism Netw., Smithsonian Institution* 19 (9). <http://dx.doi.org/10.5479/si.GVP.BGVN199409-252140>.

Gudmundsson, A., 2002. Emplacement and arrest of sheets and dykes in central volcanoes. *J. Volcanol. Geotherm. Res.* 116, 279–298.

Gudmundsson, A., 2011a. *Rock Fractures in Geological Processes*. Cambridge University Press.

Gudmundsson, A., 2011b. Deflection of dykes into sills at discontinuities and magma-chamber formation. *Tectonophysics* 500, 50–64.

Hill, D.P., 2006. Unrest in Long Valley caldera, California, 1978–2004. In: Troise, C., De Natale, G., Kilburn, C.R.J. (Eds.), *Mechanisms of Activity and Unrest at Large Calderas*. In: *Geol. Soc. (Lond.) Spec. Publ.*, vol. 269, pp. 1–24.

Hill, D.P., Dzurisin, D., Ellsworth, W.L., Endo, E.T., Galloway, D.L., Gerlach, T.M., Johnston, M.J.S., Langbein, J.O., McGee, K.A., Miller, C.D., Oppenheimer, D., Sorey, M.L., 2002. Response Plan for Volcanic Hazards in the Long Valley Caldera and Mono Craters Region California. *U.S. Geol. Surv. Bull.* 2185. 57 pp.

Itikarai, I., Kennet, B., Sinadinovski, C., 2006. Volcano-tectonic earthquakes and magma reservoirs; their influences on volcanic eruptions in Rabaul Caldera. *Earthquake Engineering in Australia*, Canberra, 24–26 November 2006.

Johnson, R.W., Itikarai, I., Patia, H., McKee, C.O., 2010. Volcanic systems of the north-eastern Gazelle Peninsula, Papua New Guinea. Rabaul Volcano Workshop Report. DMPGM Gov. Papua New Guinea and AusAID Gov., Australia. 84 pp.

Jones, R.H., Stewart, R.C., 1997. A method for determining significant structures in a cloud of earthquakes. *J. Geophys. Res.* 102, 8245–8254.

Kilburn, C.R.J., 2003. Multiscale fracturing as a key to forecasting volcanic eruptions. *J. Volcanol. Geotherm. Res.* 125, 271–289.

Kilburn, C.R.J., 2012. Precursory deformation and fracture before brittle rock failure and potential application to volcanic unrest. *J. Geophys. Res.* 117. <http://dx.doi.org/10.1029/2011JB008703>.

McKee, C.O., Lowenstein, P.L., De Saint Ours, P., Talai, B., Itikari, I., Mori, J., 1984. Seismic and ground deformation crisis at Rabaul Caldera: prelude to an eruption. *Bull. Volcanol.* 47, 397–411.

McKee, C.O., Johnson, R.W., Lowenstein, P.L., Riley, S.J., Blong, R.J., De Saint Ours, P., Talai, B., 1985. Rabaul caldera, Papua New Guinea – volcanic hazards, surveillance, and eruption contingency planning. *J. Volcanol. Geotherm. Res.* 23, 195–237.

McKee, C.O., Mori, J., Talai, B., 1989. Microgravity changes and ground deformation at Rabaul Caldera, 1973–1985. In: Latter, J.H. (Ed.), *Volcanic Hazards*. In: *IAVCEI Proc. Volcanol.*, vol. 1. Springer-Verlag, pp. 399–428.

Meredith, P.G., Main, I.G., Jones, C., 1990. Temporal variations in seismicity during quasi-static and dynamic rock failure. *Tectonophysics* 175, 249–268.

Mori, J., McKee, C., 1987. Outward dipping ring – fault structure at Rabaul Caldera as shown by earthquake locations. *Science* 235, 193–195.

Mori, J., McKee, C., Itikarai, I., Lowenstein, P.L., De Saint Ours, P., Talai, B., 1989. Earthquakes of the Rabaul seismo-deformational crisis September 1983–July 1985: seismicity on a caldera ring fault. In: Latter, J.H. (Ed.), *Volcanic Hazards*. In: *IAVCEI Proc. Volcanol.*, vol. 1. Springer-Verlag, pp. 429–462.

Nairn, I.A., McKee, C.O., Talai, B., Wood, C.P., 1995. Geology and eruptive history of the Rabaul Caldera area, Papua New Guinea. *J. Volcanol. Geotherm. Res.* 69, 255–284.

Newhall, C.G., Dzurisin, D., 1988. *Historic Unrest at Large Calderas of the World (2 volumes)*. U.S. Geol. Surv. Bull. 1855. 1108 pp.

- Parks, M.M., Biggs, J., England, P., Mather, T.A., Nomikou, P., Palamartchouk, K., Papanikolaou, X., Paradissis, D., Parsons, B., Pyle, D.M., Raptakis, P., Zacharis, V., 2012. Evolution of Santorini Volcano dominated by episodic and rapid fluxes of melt from depth. *Nat. Geosci.* 5, 749–754. <http://dx.doi.org/10.1038/ngeo1562>.
- Piochi, M., Kilburn, C.R.J., Di Vito, M., Mormone, A., Tramelli, A., Troise, C., De Natale, G., 2013. The volcanic and geothermally active Campi Flegrei caldera: an integrated multidisciplinary image of its buried structure. *Int. J. Earth Sci.* 103, 401–421. <http://dx.doi.org/10.1007/s00531-013-0972-7>.
- Pollard, D.D., Johnson, A.M., 1973. Mechanics of growth of some laccolithic intrusions in the Henry Mountains, Utah. II. *Tectonophysics* 18, 311–354.
- Saunders, S.J., 2001. The shallow plumbing system of Rabaul Caldera. A partially intruded ring fault? *Bull. Volcanol.* 63, 416–420.
- Secor, D.T., 1965. Role of fluid pressure in jointing. *Am. J. Sci.* 263, 633–646.
- Shaw, H.R., 1980. The fracture mechanisms of magma transport from the mantle to the surface. In: Hargreaves, R.B. (Ed.), *Physics of Magmatic Processes*. Princeton University, pp. 201–264.
- Smith, R., Kilburn, C.R.J., 2010. Forecasting eruptions after long repose intervals from accelerating rates of rock fracture: the June 1991 eruption of Mount Pinatubo, Philippines. *J. Volcanol. Geotherm. Res.* 191, 129–136.
- Troiano, A., Di Giuseppe, M.G., Petrillo, Z., Troise, C., De Natale, G., 2011. Ground deformation at calderas driven by fluid injection: modelling unrest episodes at Campi Flegrei (Italy). *Geophys. J. Int.* 187, 833–847.
- Troise, C., De Natale, G., Pingue, F., 1997. A model for earthquake generation during unrest episodes at Campi Flegrei and Rabaul calderas. *Geophys. Res. Lett.* 24, 1575–1578.
- Voight, B., 1988. A method for prediction of volcanic eruptions. *Nature* 332, 125–130.
- Woo, J.Y.L., Kilburn, C.R.J., 2010. Intrusion and deformation at Campi Flegrei, Southern Italy: sills, dykes, and regional extension. *J. Geophys. Res.*, 115. <http://dx.doi.org/10.1029/2009/JB006913>, 2010.
- Wood, C.P., Nairn, I.A., McKee, C.O., Talai, B., 1995. Petrology of the Rabaul Caldera area, Papua New Guinea. *J. Volcanol. Geotherm. Res.* 69, 285–302.